2021 17th International Conference on Mobility, Sensing and Networking (MSN) | 978-1-6654-0668-0/21/$31.00 ©2021 IEEE | DOI: 10.1109/MSN53354.2021.00072

RF-Vsensing: RFID-based Single Tag Contactless Vibration Sensing and Recognition

Biaokai Zhu*, Liyun Tian*, Die Wu†¶, Meiya Dong‡, Sheng Gao*, Lu Zhang*, Sanman Liu*, Deng-ao Li‡
*Shanxi Police College, Taiyuan, China
†Sichuan Normal University, Chengdu, China
‡Taiyuan University of Technology, Taiyuan, China
Emails: hongtaozhuty@gmail.com, {tian538465120, dongmeiya}@163.com, wd@sicnu.edu.cn,
vlln@qq.com, mrdeer@foxmail.com, lsm601719@126.com, lidengao@tyut.edu.cn

***Abstract*—With the rapid development of industry, vibration equipment has become one of the most widely used components for industrial systems. Utilizing vibration sensing and recognition is an effective way to diagnose and understand the working condition of these systems. However, the performance of traditional video/laser-based vibration sensing and recognition solutions varies significantly under different lighting conditions, while the invasive approaches need to directly mounting dedicated sensors to the target, which might pose a threat to its operating safety. To tackle this issue, we propose RF-Vsensing, an RFID-based contactless vibration sensing and recognition method without attaching anything to the target device. Unlike existing methods, RF-Vsensing can realize highly accurate non-contact vibration sensing and recognition using commercial off-the-shelf RFID devices. The evaluation results show that the average accuracy of vibration can reach 96.07% and the average recognition accuracy of clockwise and anticlockwise can reach 99.44%.**

***Index Terms*—RFID, Contactless, Sensing, Clockwise and anticlockwise Recognition.**

I. Introduction

The development of industry is inseparable from the normal operation of mechanical equipment. As shown in Fig. 1, mechanical equipment such as car engine [1], UAV [2], motor [3], gear [4], fan [5] usually includes a rotation module. The operation of each rotating equipment shall be maintained within a natural frequency range. Regular monitoring of the running status of rotating equipment can effectively reduce equipment failures, extend equipment lifetime, so as to reduce maintenance cost. Therefore, it is necessary to realize a equipment rotation state monitoring without affecting the normal operation of the equipment. In addition, the rotation direction is important as well. It is difficult for the equipment to withstand the impact of rotation reversal due to incomplete shutdown, which would not only prematurely damage the weak parts, but reduce the execution efficiency.

In recent years, to identify the rotation state of the vibration equipment, existing technologies mainly focus on measuring the slip, torque, vector or other indicators of the corresponding equipment. However, to obtain real-time and accurate equipment vibration information, these technologies have to mount special sensors [6] and high-precision photoelectric tachometer [7] on the equipment. As aforementioned special sensors are usually expensive, existing methods are inconvenient for pervasive deployment. Moreover, it is difficult for some equipment to bind other auxiliary instruments during operation. Therefore, for the monitoring of equipment working state, it is necessary to select non-contact vibration state identification technology to reduce the complexity of work and avoid the loss caused by stopping the equipment.

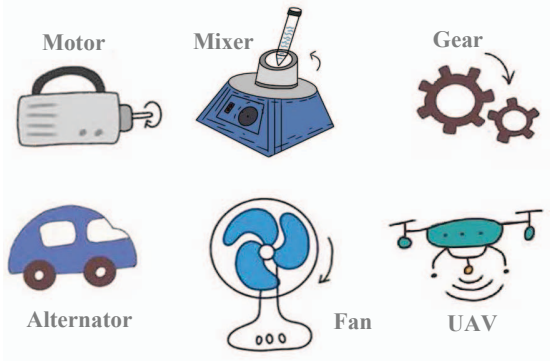

Fig. 1. Several potential vibration applications.

Nowadays, Radio Frequency IDentification (RFID) has attracted considerable attention. The existing RFID-based device sensing exploration involves various aspects, such as equipment health monitoring [8], high-speed rotation monitoring [9], [10], rotor eccentricity monitoring [11], position detection [12], etc. The success of these studies fully proves the advantages of RFID in the field of sensing and monitoring. Low-cost deployment and convenient operation have laid a solid foundation for the development of RFID. Based on this, the problem also arises: *Can we use RFID-based technology to effectively monitor the state of vibration equipment?* Through in-depth analysis, we find that it is challenging to realize contactless sensing and state recognition of vibration equipment based on RFID devices. The reasons are as follows:

- **The most simplified system deployment.** Though existing multi-tag based approaches could achieve sounds performance, sophisticated deployment is needed when

¶Corresponding author: Die Wu.

978-1-6654-0668-0/21/$31.00 ©2021 IEEE
DOI 10.1109/MSN53354.2021.00072

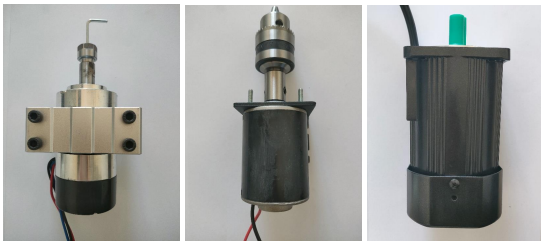

Fig. 2. Different types of vibration equipment.

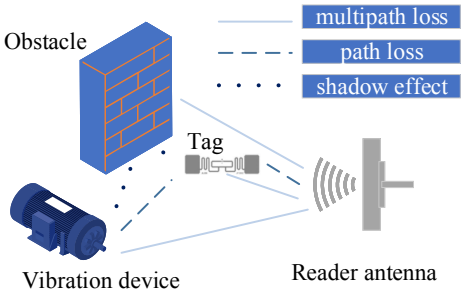

Fig. 3. Vibration sensing and recognition model.

tags are deployed. Therefore, how to reduce the number of tag deployment, so as to reduce the deployment cost and realize a non-contact sensing recognition is the first challenge.

- **High precision frequency identification.** In practical scenarios, due to the influence of various uncertain factors, the performance of traditional denoising pattern recognition is not good enough, which results in a low frequency identification accuracy. If the signal acquisition is carried out in a non-contact way, the environment, equipment and personnel will interfere with the tag's backscattered signal. Thus, how to use the weak signal to accurately identify the frequency of vibration device becomes a problem.
- **Real-time requirements.** From the perspective of received signal, there is very little difference between the clockwise and anti-clockwise rotation. In practice, we need to recognize clockwise and anti-clockwise as soon as possible so as to take measures to avoid further damage to the equipment. Therefore, how to recognize the rotation state in real time is the third challenge.

In response to the above challenges, we take the vibration equipment motors (as shown in Fig. 2) as example, and propose RF-Vsensing, a single RFID tag based contactless vibration sensing and status recognition method. In RF-Vsensing, the deployment is very simple, where we just need to place a single antenna and a single RFID tag in the vicinity of the device, and use the received signal information to perform sensing and recognition. More in detail, as the phase information of the tag is timing information, we can first remove the DC component from the phase information of the tag and realize the finite impulse response (FIR) filter through fast Fourier transform (FFT) to identify the rotation frequency of the target equipment. Secondly, we take advantage of Markov transition fields (MTF) to transform the phase signal into image features, and utilize convolutional neural network (CNN) to perform rotation state recognition. Compared with traditional machine learning method, deep learning has the advantages in image recognition, especially fine-grained feature recognition. Thirdly, to achieve real-time recognition, we propose a simplified Vgg network structure, and the evaluation result show that the model parameters and training time are greatly reduced, and the generalization ability of the model is improved.

To sum up, the main contributions of this paper are as follows:

- Our approach is a contactless approach that we can realize real-time monitoring without mount anything to the target equipment, i.e., we only need to place a single RFID tag and single antenna in the vicinity of the target device.
- We adopt the feature recognition model of tag phase signal based on Markov transition method. The model can transform the phase information of the tag into a Markov transition diagram, and realize the real-time monitoring of anomaly positive and negative identification.
- RF-Vsensing can realize the rotation identification of various vibration equipment. We use commercial readers and tags to simplify scenario deployment. The average accuracy of rotation frequency recognition, clockwise and anti-clockwise recognition are 96.07% and 99.44% respectively. All these verify the excellent performance of the system.

II. Preliminaries

A. Vibration sensing model

In RFID system, the tag's phase information will be influenced when the nearby rotation equipment is operating. In our work, the vibration sensing model is shown in the Fig. 3. It consist of an RFID tag, an RFID reader antenna, and a target vibration device. In practice, the phase information is often mixed with multipath loss, path loss, and shadow effects.

In the process of transmission, the vibration signal of the motor and other equipment will be reflected through the actual environment and obstacles. The uncontrollable changes in the length of these transmission paths will cause the differences in the receiving time, phase and other parameters of the signals in each path. This difference will make the phase signal superimpose, and then produce the common multipath fading phenomenon. Among these signals, RSSI and Doppler are sensitive to the change of relative position. In the case of non-contact between the tag and the equipment, the vibration frequency of the equipment can be identified by the in-depth processing of the tag phase information.

B. Non-contact clockwise and anti-clockwise identification

The signal information collected by commercial readers includes RSSI and Doppler which are easily affected by the environment. We can only select the phase information to identify and analyze the positive and negative rotation. However, due to the unique property of phase angle difference π between positive and negative, we have extracted the key to solve the problem. We transform the phase information of tags into images of Markov transition field, and then use convolution neural network model in deep learning to identify the differences of images in Markov field.

Convolution neural network with deep learning can be regarded as a combination of a series of processing. The initial combination of convolution layer and sampling layer has different functions. The convolution layer contains multiple convolution cores which are equivalent to multiple filters and can output multiple corresponding feature maps. Each image will also be the output unit, which is output by convolution layer, and then the obtained characteristic image can be transferred by nonlinear activation function. In this way, by combining the features of adjacent positions of different layers, the detected local features can be formed. The sampling layer can integrate the features. Even small features can be input into the orientation of the feature map by sampling, which greatly reduces the size of the feature map.

III. System Design

A. Signal acquisition

For ease of deployment, we use a commercial off-the-shelf reader to extract the tag signal. Commercial reader do not provide the underlying data interface, especially the physical layer data that tags communicate with readers. The tag reflection signal received by commercial reader only contains the following data: received signal strength indication, phase angle value, Doppler shift data. The value of these reflected signals will change with the change of tag position, moving speed and surrounding environment.

In order to improve the weak electromagnetic signals that the reader receives from the tag as much as possible, the system uses a circularly polarized antenna. The antenna has large volume and high gain, which can make up for the attenuation of high strength signal caused by distance, and minimize the loss of signal energy received by the tag and the reader. Wherein, the power received by the tag and the power received by the reader are expressed as follows:

$$P_{R\_tag} = P_{T\_reader} G_{reader} G_{tag} \alpha \left(\frac{\lambda}{4\pi d}\right)^2 \quad (1)$$

$$P_{R\_reader} = \beta P_{T\_reader} G_{reader}^2 G_{tag}^2 \alpha^2 \left(\frac{\lambda}{4\pi d}\right)^4 \quad (2)$$

In the above formula, β denotes the utilization rate of the energy emitted by the reader, P_{T_reader} is the power transmitted by the reader, G_{reader} is the gain of the reader antenna, G_{tag} is the gain of the tag, α is the attenuation coefficient of the propagation channel between the reader and the tag, λ is the radio electromagnetic wave length, and d is the communication distance between tag and reader.

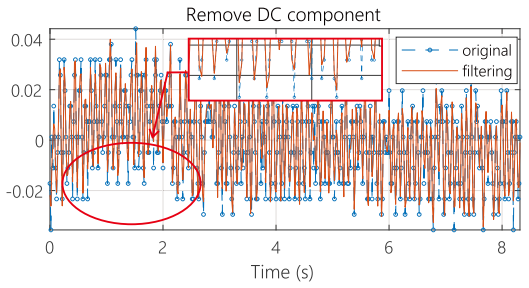

(a) Remove DC component

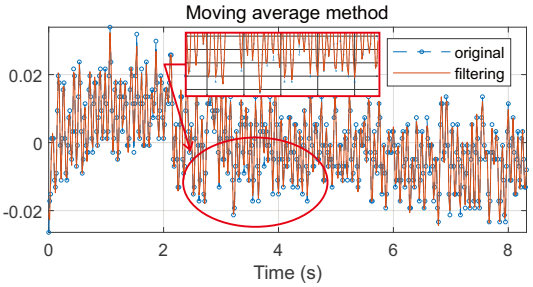

(b) Moving average method

Fig. 4. Comparison of denoising methods.

B. Signal denoising

In the process of signal transmission and acquisition, the interference introduced by the external environment and the noise produced by itself will have a significant influence on the received signal. Even a small noise will have a huge impact on the analysis results. Therefore, we should first consider how to purify the data, that is, to remove the noise from the received signal.

We compare the DC component denoising and moving average denoising methods. The DC component of the signal is the average value of the signal, which is a constant independent of time. The DC component of the signal can be expressed as follows:

$$f_{DC} = \lim_{T\to\infty} \frac{1}{2T} \int_{-T}^{T} f(t)dt \quad (3)$$

The moving average method gives weight to the signal information, with large coefficient given to the recent data and small coefficient given to the long-term data, so as to eliminate the variable factors of the signal information. Before performing signal denosing, the original phase signal is smoothed to reduce the impact of data mutation. In order to obtain better actual denoising effect, the smoothing factor of the moving average method was set as 0.3 in the experimental setting. During this period, we found that if the value is

too large, the key characteristic values of the signal will be lost, and if the value is too small, the smoothness will be incomplete. In our approach, we select the 0.3 as the value of smoothing factor.

By comprehensively comparing Fig. 4(a) (DC component removal method) and Fig. 4(b) (Moving average method), we find that the DC component removal method retains the tag phase information, and the phase curve is smoother as well, moreover, the denoised curve has less jitter. Therefore, our approach adopt DC component removal method to perform signal denoise.

C. Vibration frequency sensing

The sampling rate of commercial readers is low, usually up to 40 Hz. According to Nyquist's sampling theorem and practical engineering results, we choose a Finite Impulse Response (FIR) filter implemented by FFT for filtering and vibration frequency identification. FIR low-pass filter can retain the phase frequency characteristics on the basis of ensuring any amplitude frequency characteristics, and the unit sampling response is limited, so the system can maintain a relatively stable effect. The phase information of tag is easy to be disturbed by environmental noise, so a stable identification system is particularly important for vibration identification of equipment in complex environment.

FIR filter is a kind of approximation based on the frequency characteristics of ideal filter. It adopts the method of window function and sampling response of unit frequency to approach continuously. Assuming that the cut-off frequency of low-pass digital filter is $w_{cut-off}$ and the group delay is α, the unit impulse of filter should be expressed as follows:

$$h_d(n) = \frac{1}{2\pi} \int_{-\pi}^{\pi} H_d(e^{jw}) e^{jw} dw \tag{4}$$

Further derivation of the above formula shows that:

$$h_d(n) = \frac{\sin(w_c(n-a))}{\pi(n-a)} \tag{5}$$

The unit impulse response of the ideal filter is infinite, but in practical application, the length of the low-pass filter is finite, so it is necessary to choose a better Hanning window function to adjust $h_d(n)$. According to the function selection, the system achieves high precision vibration frequency perception.

D. Clockwise and anti-clockwise recognition

In our approach, three signal indicators received by commercial readers are analyzed. RSSI value is sensitive to the change of location and is easily affected by the environment. Slight changes in Doppler values are difficult for commercial reader to pick up. For this reason, we carried out a deep excavation of tag phase information. The actual difference between the forward rotation and reverse rotation of the equipment is analyzed from the perspective of phase, and phase signal is actually belong to one-dimensional time series signal. Therefore, the phase information of tags is abstracted as a time series classification problem.

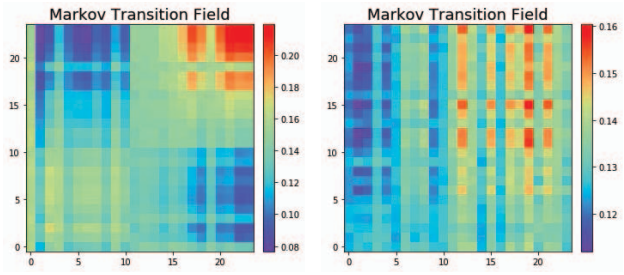

(a) Clockwise rotation (b) Anti-clockwise rotation

Fig. 5. Markov Transition Field.

The tag phase information received by the reader antenna is a random variable and is arranged in chronological order. The distribution characteristic at time $t+1$ has nothing to do with the random variables before time t, which conforms to the Markov property.

Suppose the time series $T = \{t_1, t_2, \ldots, t_N\}$, we divide the range into Q series, each t_i in the time series information is mapped to the corresponding q_i, through continuous mapping, we can get a matrix $Q*Q$ of W, w_{ij} represents the generalization that the j element in the sequence is followed by the i element in the sequence, that is, $w_{ij} = P(a_t \in q_i \,|a_{t-1} \in q_j)$, and satisfies $\sum_{j=1}^{Q} w_{ij} = 1$. So we can get the matrix $W=(w_{ij})_{1\leq i,j\leq Q}$. Let the transition matrix M, where m_{ij} denotes the probability of the transition from Z to Q, where V = 1 Let the transition matrix M, where m_{ij} denotes the probability $P(q_i \to q_j)$ of the transition from i to j in the sequence, where $\sum_{1\leq j\leq Q} m_{ij} = 1$.

The random field contains two important characteristics: position and phase space. After the phase space is assigned to each position according to the random distribution, the value in any position is only related to the adjacent position, and has nothing to do with other positions. Using this feature, we transform the tag phase angle information in accordance with time series into Markov Transition Field (MTF). We take the MTF of normal and reverse rotation as an example (as shown in Fig. 5).

From Fig. 5(a) and Fig. 5(b), it is difficult to extract the characteristic information of the image. Deep neural network can learn input sample data layer by layer and extract data features from the details of image information. Among them, Convolutional Neural Networks (CNN) is widely used in the field of image recognition. CNN can overcome the shortcomings of traditional signal processing, especially for the recognition of small features. The core of convolution neural network is to extract features through larger convolution kernel. For example, alexnet, resnet18, etc. The larger the size of convolution kernel, the stronger the ability to explore information features. In this way, more parameters will be introduced, and the computational complexity will be improved. VGG network uses 3×3 convolution kernels in each block instead of large convolution kernels, and uses three 3×3

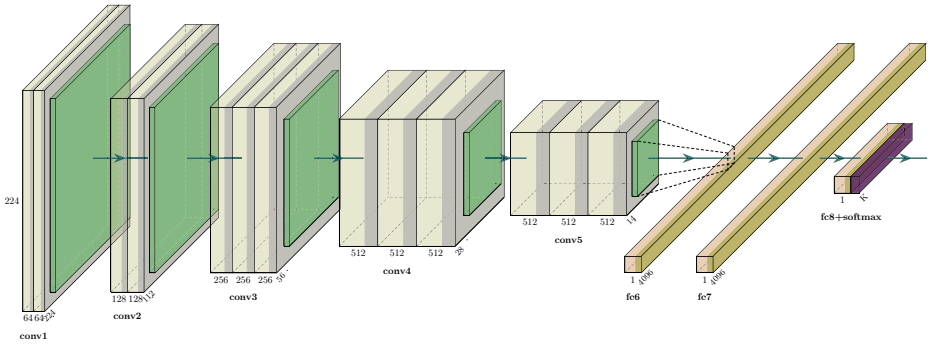

Fig. 6. Vgg16 network model.

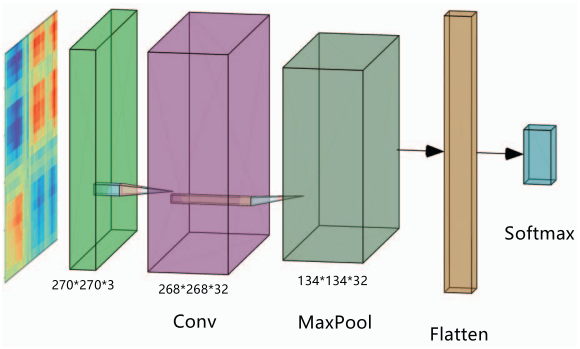

Fig. 7. Simplified VGG model.

convolution kernels to be equivalent to the receptive field of 7×7 convolution kernels, but the parameters are reduced by nearly half.

The original Vgg model can have as many as 16 layers, 13 convolution layers and 3 fully connected layers, and can output 1000 classifications. The specific parameters are as follows: the size of convolution kernel is 3×3, the step size is 1, and the padding of convolution is 2. The size of pooling layer is 2×2, and the step size is 2. Each layer contains 4096 neurons. Softmax layer is used in the output layer and ReLU is used in the activation function. The Vgg model as depicted in Fig. 6.

We use image data generator to preprocess the image. The rotated image is not clipped to avoid errors due to compression. The original image is 270×270 pixels. After loading, the image is normalized, and the pixel value is reduced to between 0 and 1, which is conducive to the convergence of the model and avoids the "death" of neurons. In this paper, the image inversion is mainly composed of two parts: positive phase and reverse phase. In order to improve the computing speed and reduce the complexity of the model, we simplify the VGG model step by step.

We summarize the proposed model. Firstly, the input data is 270×270 training image. After a 3×3 convolution kernel and 32 filters, we output $268 \times 268 \times 32$ dimensional matrix. Then, after a 2×2 maximum pooling layer, we output $134 \times 134 \times 32$ dimensional data. After a series of feature extraction,

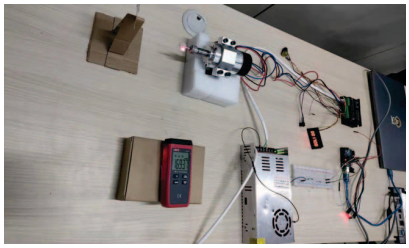

(a) Overall

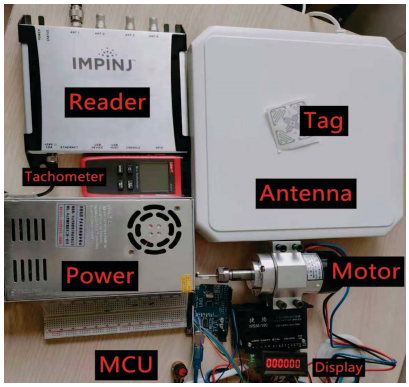

(b) Experiment setup

Fig. 8. Experiment scene and setup.

we flatten the matrix through the Flatten layer and eventually input it into a model of 32 neurons, achieving the output of Softmax activating the two classifications (as depicted in Fig. 7).

IV. System Implementation

Hardware: In the experiment, we use the Impinj Speedway R420 reader, which adopts the EPC Gen2 standard, and its working frequency band is between 920 and 925 MHz. It selects Max throughput in the working mode, so that the measured value can reach the maximum throughput. In order to maximize the number of observed samples, llrp protocol tags are used to communicate with readers. We use RFID directional antenna. Finally, we also use single-chip

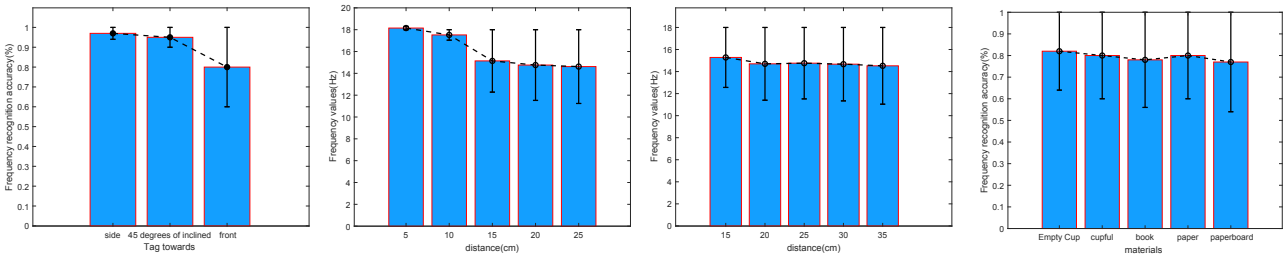

(a) Tag orientation (b) Impact of T-M distance (c) Impact of T-A distance (d) Effect of blockage

Fig. 9. Comparison of multiple factors.

microcomputer, tachometer, in order to control the speed and direction of the motor. At the same time, we can also measure and display the motor speed. The reader can receive the RSSI, Phase, Doppler and other information of the tag, and synchronously transmit it to the laptop for processing and monitoring.

Software: In this experiment, we use the embedded Impinj LLRP toolkit to communicate with the reader. Impinj reader improves this protocol to support phase reading report. For the client software, we use C#, and then realize the network connection. In the overall experiment, we are equipped with Intel i5-8265u CPU and 8G RAM Lenovo PC, which makes the software implementation compatible with LLRP toolkit, and simply and directly obtain the tag information from the reader.

Experiment scene: These devices take the frequency data converted by manual adjustment of motor speed as the basis to carry out a series of explorations. The instrument deployment includes R420 reader, directional antenna, tag, motor, MCU, tachometer, Lenovo PC and other equipment (as shown in Fig. 8). These devices can realize real-time vibration sensing and recognition. Through actual scene deployment, they not only innovate and intelligentize the traditional mode, but also lay a foundation for realizing the efficient recognition of industrial equipment vibration sensing.

Implementation: In this experiment, the maximum sampling rate that can be realized is 80Hz, but in this case, the placement distance between the tag and the reader is too small, which is inconsistent with the reality. In order to be more in line with the reality, we chose a sampling rate of 60Hz with a better effect for the experiment. In the process of single-chip adjusting motor speed, the maximum can reach 3600RPM per minute.

V. Performance Evaluation

Tag orientation: In the experiment, we compare the tag with the motor in forward direction, 45 degrees and side direction, and observe the accuracy of tag recognition in three different directions. Fig. 9(a) shows the effect of tag orientation on the accuracy of frequency recognition. It can be seen from this that if the tag and the reader are in positive correspondence, that is, the tag is placed sideways with the motor, the accuracy of frequency identification is the highest.

Influence of distance between tag and motor: We change the distance between the tag and the reader from 5cm to 25cm. From Fig. 9(b), we can see that when the distance between the tag and the motor is too large, the reflected signal becomes weak and the recognition accuracy is reduced. In order to further improve the experimental accuracy and sensing range, we can select a more effective directional antenna to concentrate energy.

Influence of distance between tag and antenna: We change the distance between the tag and the antenna from 15 to 35 cm. Fig. 9(c) depicts that as the distance between the tag and the antenna increases, the error increases correspondingly. In order to achieve the best recognition performance, we keep the distance between the antenna and the tag at about 15cm to improve the recognition accuracy.

Effect of blockage: In this experiment, we performed relevant operations in the challenging NLOS (non-line-of-sight), such as: Objects of different materials (empty water cup, full water cup, book, paper, cardboard) are used to block the signal transmission between the tag and the reader respectively. During the experiment, attention should be paid to keeping the distance between the tag, motor and antenna constant. Under this condition, it can be clearly seen from the Fig. 9(d) that blocking has a great impact on the recognition accuracy of frequency and clockwise and anti-clockwise rotation, which greatly reduces the accuracy of frequency recognition. However, it can be seen from the figure that the recognition accuracy is still around 0.8, and the error is within a certain range, which provides a great possibility for the deployment in the specific experimental environment.

Identification accuracy of different vibration frequencies: During the experiments, we adjust the frequency of the vibration equipment through the single chip microcomputer, process the extracted data with filters, and test its final perception performance. Fig. 10 describes the sensing accuracy at different frequencies (taking 8Hz to 17Hz as an example). It can be seen from the figure that the best sensing accuracy can be achieved at 16Hz and the average accuracy has reached 96.07% at different frequencies.

Clockwise and anticlockwise recognition accuracy of

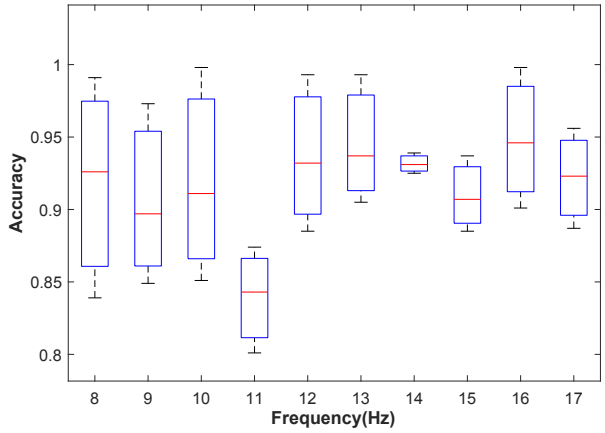

Fig. 10. Different frequency sensing accuracy.

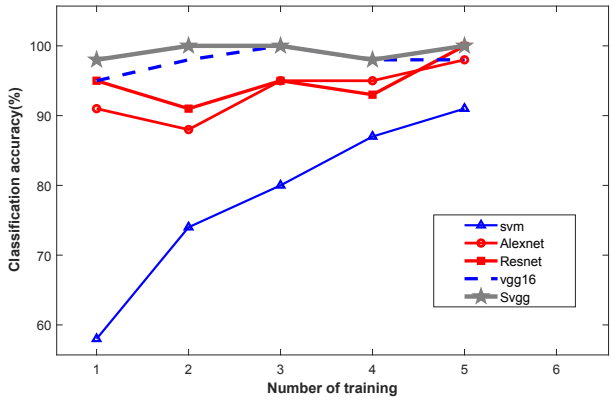

Fig. 11. Training iterations and recognition accuracy.

different network models: In the experiment, machine learning and deep learning methods were respectively used to test performance (SVM, Alexnet, Resnet, Vgg16, SVgg). As can be seen from Fig. 11, the recognition accuracy of traditional SVM is low, while the accuracy of the improved Deep learning SVgg model is high, with an average accuracy of 99.44%.

Other factors: We still conduct experiments and identify frequencies in the multipath environment, but it can be clearly found that under the condition of strong multipath, phase values overlap with each other and interfere with each other, resulting in original signal distortion and even errors, thus greatly reducing the accuracy of frequency recognition.

Challenging Scenarios: In order to assess the maximum universality of the system, more challenging scenarios need to be experimented in later studies. Now we preliminarily set the subsequent experiment scene in the vibration equipment such as fan, engine and gyro. The use of tags, antennas and other equipment for real-time monitoring of frequency and rotation direction, effectively maximize the utilization of the system, convenient for production and life.

VI. RELATED WORK

Special sensor-based methods: In traditional contact vibration monitoring and positive and negative rotation identification, the use of sensors has attracted a lot of attention of researchers. Liu et. al uses Kinect sensor V2 and artificial neural network to measure vibration frequency [13]. Bhardwaj et. al proposed a laser sensor [14] based on self-mixing optical feedback interference technology to measure micro-harmonic vibration. Spirin et. al proposed that a semiconductor laser could replace the standard reference oscillator of a coherent reflectometer in a distributed fiber optic vibration sensor system [15] to measure the vibration frequency. Li et. al designed a low-frequency vibration monitoring system [16] in which the grating sensor was installed in a specific device to obtain the vibration signal of the hydraulic generator.

Video image-based methods: Aiming at the problem that traditional vision cannot extract high frequency vibration signal, Ferrer et. al further measured the vibration frequency by using camera with high acquisition rate, image acquisition and multistage threshold segmentation technology [17]. Wang et. al [18] proposed that different vibration spatial information can be recorded in frame images by RGB-D camera and can be combined with depth to monitor low-frequency vibration. Gorjup et. al proposed a full-field 3D measurement of high-frequency vibration using a monochrome camera of still frame [19], which effectively reduced the recognition and processing time. Jiang et. al proposed a vision-based vibration source capture method to extract vibration image regions in high frame rate videos using pixel-level digital filters [20].

Laser measuring equipment-based methods: This method has the advantages of wide range, high accuracy and non-contact, etc., not only has very high application value, but also has attracted widespread attention in the industry. Yamaguchi et. al proposed a vibration measurement system [21] of pulsed optical fiber Bragg Grating, which is similar to pulse sequence to separate and monitor reflected signals, so as to achieve the purpose of multi-point real-time vibration measurement. Bhardwaj et.al proposed a new method [22] for solving SM-OFI signals using multi-objective composite mutation genetic algorithm, which achieved the purpose of simultaneous measurement of absolute distance and frequency of vibration.

Time-frequency domain analysis-based methods: The fault information in vibration signal is often presented in weak frequency band, and frequency band identification method can be used to enhance the weak fault information in vibration signal, so researchers often transform the signal into monitoring in time-frequency domain. Pan et. al proposed the inversion of the optimal model parameters in the time domain or frequency domain and the combination of Bayes to achieve the purpose of fracture property monitoring [23]. Schmidt et. al proposed a frequency band identification method based on optimization [24], which enabled the system not only to enhance the ability of fault information, but to be used for automatic fault detection under time-varying conditions.

RFID-based methods: RFID technology has achieved real-

time positioning tracking [25] [26], gesture recognition [27], drop speed detection [28], industrial health awareness [29] [30], etc. Moreover, Tagbeat [9] mounts RFID tags on the target device to sense vibration frequency, and TagSound [31] also innovatively uses the signal changes caused by tags to detect vibration frequency.

VII. Conclusion

In this paper, we propose RF-VSensing, a single tag vibration sensing and state recognition system based on RFID. The system not only realizes non-contact vibration frequency sensing, but also realizes real-time clockwise and anti-clockwise rotation recognition. The evaluation results show that the average precision of vibration sensing and recognition can reach 96.07% and 99.44% respectively, which effectively breaks the traditional general mode. Based on this, we believe that RF-VSensing will be very suitable for sensing and state recognition of multiple types of vibration equipment in the future.

Acknowledgment

The research is supported by National Natural Science Fund China (No. 62002250, 62072320), Education Innovation Fund of Ministry (No. 2019J02009), Scientific and Technologial Innovation Programs of Higher Education Institutions in Shanxi (No. 2019L1009). We thank all the anonymous reviewers for their valuable comments and helpful suggestions.

References

[1] J. Chen, H. Guo, G. Liu, X. Wang, Y. Xi, M. S. Javed, and C. Hu, "A fully-packaged and robust hybridized generator for harvesting vertical rotation energy in broad frequency band and building up self-powered wireless systems," *Nano Energy*, vol. 33, pp. 508–514, 2017.

[2] Z. Jingcheng, F. Xinru, Y. Zongkai, and X. Fengtong, "Uav detection and identification in the internet of things," in *International Wireless Communications & Mobile Computing Conference (IWCMC)*. IEEE, 2019.

[3] X. Run and C. Zhiqing, "Technological analysis on motor stall and its perspective," *Electrical Science & Engineering*, vol. 2, no. 1, pp. 26–29, 2020.

[4] S. Xue and I. Howard, "Torsional vibration signal analysis as a diagnostic tool for planetary gear fault detection," *Mechanical Systems and Signal Processing*, vol. 100, pp. 706–728, 2018.

[5] C. S. Alex, L. Huang-Chang, C. Yu-Chieh, L. Tien-Hua, C. H. Simon, H. Lung-Hsien, H. Chih-Wei, H. Yih-Shiou, L. Jiann-Der, and C. Chih-Hsiung, "Design and implementation of acoustic sensing system for online early fault detection in industrial fans," *Journal of Sensors*, vol. 2018, pp. 1–15, 2018.

[6] X. Xu, X. Tian, and L. Zhou, "A robust incremental-quaternion-based angle and axis estimation algorithm of a single-axis rotation using marg sensors," *IEEE Access*, vol. 6, pp. 42 605–42 615, 2018.

[7] Q. Yang, J. Liu, H. Guo, X. Zeng, and W. Hu, "A novel design of information collection system for vehicles for real-time monitoring," in *IEEE Conference on Industrial Electronics and Applications (ICIEA)*. IEEE, 2019.

[8] P. Yang, Y. Feng, J. Xiong, Z. Chen, and X.-Y. Li, "Rf-ear: Contactless multi-device vibration sensing and identification using cots rfid," in *IEEE INFOCOM 2020-IEEE Conference on Computer Communications*. IEEE, 2020, pp. 297–306.

[9] L. Yang, Y. Li, Q. Lin, H. Jia, X.-Y. Li, and Y. Liu, "Tagbeat: Sensing mechanical vibration period with cots rfid systems," *IEEE/ACM transactions on networking*, vol. 25, no. 6, pp. 3823–3835, 2017.

[10] P. Li, Z. An, L. Yang, and P. Yang, "Towards physical-layer vibration sensing with rfids," in *IEEE INFOCOM 2019-IEEE Conference on Computer Communications*. IEEE, 2019, pp. 892–900.

[11] Y. He, Y. Zheng, M. Jin, S. Yang, X. Zheng, and Y. Liu, "Red: Rfid-based eccentricity detection for high-speed rotating machinery," *IEEE Transactions on Mobile Computing*, 2019.

[12] B. Xie, J. Xiong, X. Chen, and D. Fang, "Exploring commodity rfid for contactless sub-millimeter vibration sensing," in *Proceedings of the 18th Conference on Embedded Networked Sensor Systems*, 2020, pp. 15–27.

[13] J. Liu and X. Yang, "Artificial neural network for vibration frequency measurement using kinect v2," *Shock and Vibration*, vol. 2019, 2019.

[14] V. K. Bhardwaj and S. Maini, "Measurement of micro-harmonic vibration from optical feedback interferometry using wavelet trend analysis," *Optics communications*, vol. 476, p. 126330, 2020.

[15] V. Spirin, C. López-Mercado, M. Wuilpart, D. Korobko, I. Zolotovsky, and A. Fotiadi, "Using a semiconductor laser with frequency capture as an operating optical generator of a coherent reflectometer for distributed vibration frequency measurements," *Instruments and Experimental Techniques*, vol. 63, no. 4, pp. 476–480, 2020.

[16] S. Li, L. Min, X. Zhang, F. Zhang, Z. Sun, and M. Wang, "Application of fbg sensor for low frequency vibration monitoring in hydroelectric generating," in *2018 IEEE 3rd Optoelectronics Global Conference (OGC)*. IEEE, 2018, pp. 102–105.

[17] B. Ferrer, J. Espinosa, A. B. Roig, J. Perez, and D. Mas, "Vibration frequency measurement using a local multithreshold technique," *Optics express*, vol. 21, no. 22, pp. 26 198–26 208, 2013.

[18] W. Wang, D. Yang, and J. Shi, "Low-frequency sound prediction of structures with finite submerge depth based on sparse vibration measurement," *Applied Sciences*, vol. 11, no. 2, p. 768, 2021.

[19] D. Gorjup, J. Slavič, A. Babnik, and M. Boltežar, "Still-camera multiview spectral optical flow imaging for 3d operating-deflection-shape identification," *Mechanical Systems and Signal Processing*, vol. 152, p. 107456, 2021.

[20] M. Jiang, Q. Gu, T. Aoyama, T. Takaki, and I. Ishii, "Real-time vibration source tracking using high-speed vision," *IEEE Sensors Journal*, vol. 17, no. 5, pp. 1513–1527, 2017.

[21] T. Yamaguchi, Y. Sugimoto, and Y. Shinoda, "Development of real-time vibration measurement system by fiber bragg gratings with pulse light," *Electronics and Communications in Japan*, vol. 103, no. 11-12, pp. 9–15, 2020.

[22] B. Vkba and A. Sm, "Estimation of absolute distance and high-frequency vibration from the modulated sm-ofi signal using compound mutated genetic algorithm," *Optics and Lasers in Engineering*, vol. 134.

[23] X. Pan, D. Zhang, and P. Zhang, "Fracture detection from azimuth-dependent seismic inversion in joint time–frequency domain," *Scientific Reports*, vol. 11, no. 1, pp. 1–15, 2021.

[24] S. Schmidt and K. C. Gryllias, "Combining an optimisation-based frequency band identification method with historical data for novelty detection under time-varying operating conditions," *Measurement*, vol. 169, p. 108517, 2021.

[25] C. Wang, L. Xie, K. Zhang, W. Wang, Y. Bu, and S. Lu, "Spin-antenna: 3d motion tracking for tag array labeled objects via spinning antenna," in *IEEE INFOCOM 2019-IEEE Conference on Computer Communications*. IEEE, 2019, pp. 1–9.

[26] L. Yang, Q. Lin, X. Li, T. Liu, and Y. Liu, "See through walls with cots rfid system!" in *Proceedings of the 21st Annual International Conference on Mobile Computing and Networking*, 2015, pp. 487–499.

[27] S. Pradhan, E. Chai, K. Sundaresan, L. Qiu, M. A. Khojastepour, and S. Rangarajan, "Rio: A pervasive rfid-based touch gesture interface," in *Proceedings of the 23rd Annual International Conference on Mobile Computing and Networking*, 2017, pp. 261–274.

[28] X. Liang, B. Lin, Z. Liu, and A. Du, "Analysis of amplitude and frequency detection error of surface acoustic wave generated by laser line source," *Applied Acoustics*, vol. 177, p. 107934, 2021.

[29] C. Duan, L. Yang, Q. Lin, Y. Liu, and L. Xie, "Robust spinning sensing with dual-rfid-tags in noisy settings," *IEEE Transactions on Mobile Computing*, vol. 18, no. 11, pp. 2647–2659, 2018.

[30] L. Yang, Y. Li, Q. Lin, X.-Y. Li, and Y. Liu, "Making sense of mechanical vibration period with sub-millisecond accuracy using backscatter signals," in *Proceedings of the 22nd Annual International Conference on Mobile Computing and Networking*, 2016, pp. 16–28.

[31] P. Li, Z. An, L. Yang, P. Yang, and Q. Lin, "Rfid harmonic for vibration sensing," *IEEE Transactions on Mobile Computing*, 2019.